FLORES, P., AMBRÓSIO, J., CLARO, J.C.P., LANKARANI, H.M., TRANSLATIONAL JOINTS WITH CLEARANCE IN RIGID MULTIBODY SYSTEMS. ASME JOURNAL OF COMPUTATIONAL AND NONLINEAR DYNAMICS, VOL. 3(1), PP. 0110071-10, 2008 (DOI: 10.1115/1.2802113)

P. Flores *
Departamento de Engenharia Mecânica
Universidade do Minho, Campus de Azurém
4800-058 Guimarães Portugal
Phone: + 351 253510220; Fax: + 351 253516007
E-mail: pflores@dem.uminho.pt

J. Ambrósio
Instituto de Engenharia Mecânica (IDMEC)
Instituto Superior Técnico
Av. Rovisco Pais 1, 1049-001 Lisboa Portugal
Phone: + 351 218417680; Fax: + 351 218417915
E-mail: jorge@dem.ist.utl.pt

J.C.P. Claro
Departamento de Engenharia Mecânica
Universidade do Minho, Campus de Azurém
4800-058 Guimarães Portugal
Phone: + 351 253510221; Fax: + 351 253516007
E-mail: jcpclaro@dem.uminho.pt

H.M. Lankarani
Department of Mechanical Engineering,
Wichita State University,
Wichita, KS 67260-133
Phone: 316 9783236, Fax : 316 9783236
E-mail: hamid.lankarani@wichita.edu

ABSTRACT

A computational methodology for dynamic description of rigid multibody systems with translational clearance joints is presented and discussed in this work. Over the last years, extensive work has been done to study the dynamic effect of the revolute joints with clearance in multibody systems, in contrast with the little work devoted to model translational joints with clearance. In a joint with translation clearance there are many possible ways to set the physical configuration between the slider and guide, namely: (i) no contact between the two elements, (ii) one corner of the slider in contact with the guide surface, (iii) two adjacent slider corners in contact with the guide surface, (iv) two opposite slider corners in contact with the guide surfaces. The proposed methodology takes into account these four different situations. The conditions for switching from one case to another depend on the system dynamics configuration. The existence of a clearance in a translational joint removes two kinematic constraints from a planar system and introduces two extra degrees of freedom in the system. Thus, a translational clearance joint does not constrain any degree of freedom of the mechanical system

* Corresponding author

but it imposes some restrictions on the slider motion inside the guide limits. When the slider reaches the guide surfaces an impact occurs and the dynamic response of the joint is modeled by contact-impact forces. These forces are evaluated here with continuous contact force law together with a dissipative friction force model. The contact-impact forces are introduced into the system's equations of motion as external generalized forces. The proposed methodology is applied to a planar multibody mechanical system with a translational clearance joint in order to demonstrate its features.

Keywords: Clearance Joints, Multibody Dynamics, Contact-impact Forces

1. INTRODUCTION

The traditional dynamic analysis of rigid multibody systems has inherent limitations since the kinematic joints are not modeled taking into account their physical characteristics but instead as ideal kinematic constraints. Consequently, factors like clearance, friction, local elastic/plastic deformations and bodies' flexibility are not considered. In reality, the multibody systems are connected by kinematic joints in which some clearance is always present. That clearance is indispensable to permit a correct functioning of the pair elements. Causes of clearance in multibody systems have been identified as being due to the manufacturing process, local deformation, thermal effects and wear. The clearances always cause collision between the elements that compose the clearance joints and, consequently, impact forces are developed and transmitted throughout the multibody system.

Over the last few decades, extensive work has been done to study the dynamic effect of the revolute and spherical joints with clearance in multibody systems [1-6]. However, most of these works are referred to unlubricated joints. Bauchau and Rodriguez [7] and Flores et al. [8] are among the few who have incorporated the lubrication effect at the clearance joints in the simulation of multibody systems. In these works the mechanical systems used to demonstrate the proposed approaches are four bar linkage and slider crank mechanisms. In contrast to the revolute and spherical clearance joints, little work has been developed to model translational joints with clearance. Wilson and Fawcett [9] derived the equations of motion for the different scenarios of the slider motion inside the guide. They also showed how the slider motion in a translational clearance joint depends on the geometry, speed and mass distribution. Farahanchi and Shaw [10] studied the dynamic response of a planar slider-crank mechanism with slider clearance. They demonstrated how complex the system's response is, which can be chaotic or periodic. More recently, Thümmel and Funk [11] used the complementary approach to model impact and friction in a slider-crank mechanism with both revolute and translational clearance joints.

The primary aim of this work is to present a computational methodology for dynamic description of rigid multibody systems with translational clearance joints. In the present work, the slider and the guide elements that constitute a translational clearance joint are modeled as two colliding bodies and the dynamics of the joint is

governed by contact-impact forces. The modeling of translational clearance joints is more complicated than that for the revolute joints, because in a translational clearance joint there are many possible ways to set the physical configuration between the slider and guide, namely: (i) no contact between the two elements, (ii) one corner of the slider in contact with the guide surface, (iii) two adjacent slider corners in contact with the guide surface, (iv) two opposite slider corners in contact with the guide surfaces. The conditions for switching from one case to another depend on the system dynamics configuration. The proposed methodology takes into account these four different situations.

A translational clearance joint does not constrain any degree of freedom from the mechanical system as an ideal joint, but it imposes some restrictions on the slider motion inside the guide limits. When the slider reaches the guide surfaces an impact occurs and the dynamic response of the joint is modeled by contact-impact forces. These forces are evaluated according to a continuous contact force law [12] together with a dissipative friction force [13]. Then these contact forces are added into the system's equations of motion as external generalized forces [14]. The dynamic system's response is obtained by numerically solving the system's equations of motion and contact-impact forces produced by the collision between the slider and guide. The initial conditions necessary to start the integration process are obtained from kinematic simulation of the mechanical system in which all the joints are considered to be ideal. The Baumgarte stabilization technique is used to control the position and velocity constraint violations [15]. Furthermore, the integration process is performed by employing a predictor-corrector algorithm with variable time step and variable order [16,17]. Finally, a planar multibody mechanical system is used as numerical example to discuss the assumptions and procedures adopted throughout this work.

2. MULTIBODY DYNAMICS FORMULATION

A multibody system is a collection of bodies that is acted upon by forces and moments. These bodies are interconnected to each other by different types of kinematic joints that constrain their relative motion in different forms. The formulation of multibody system dynamics adopted here follows closely the Nikravesh's work in which the generalized Cartesian coordinates are used to describe the system configuration [14].

For a constrained multibody system the kinematic joints can be described by a set of linear and/or nonlinear holonomic algebraic equations as

$$\boldsymbol{\Phi}(\mathbf{q}, t) = \mathbf{0} \qquad (1)$$

where $\mathbf{q}$ is the generalized coordinates vector and t is the time variable. Differentiating Eq. (1) with respect to time yields the velocity constraint equation. After a second differentiation with respect to time the acceleration constraint equation is obtained

$$\boldsymbol{\Phi}_{\mathbf{q}}\ddot{\mathbf{q}} = \boldsymbol{\gamma} \qquad (2)$$

in which $\boldsymbol{\Phi}_{\mathbf{q}}$ is the Jacobian matrix of the constraint equations, $\ddot{\mathbf{q}}$ is the acceleration vector and $\boldsymbol{\gamma}$ is the right hand side of acceleration equations, which contains the terms that are exclusively function of velocity, position and time.

The translational and rotational equations of motion for an unconstrained multibody system of rigid bodies are written as

$$\mathbf{M}\ddot{\mathbf{q}} = \mathbf{g} \qquad (3)$$

where $\mathbf{M}$ is the global system mass matrix, containing the mass and moments of inertia of all bodies, and $\mathbf{g}$ is the generalized force vector that contains all external forces and moments applied on the system.

Using the Lagrange multipliers technique the constraint equations (1) is added to the equations of motion (3). Thus, the equations of motion are written together with the second time derivative of constraint equations (2) yielding a system of equations written as

$$\begin{bmatrix} \mathbf{M} & \mathbf{\Phi}_{\mathbf{q}}^{T} \\ \mathbf{\Phi}_{\mathbf{q}} & \mathbf{0} \end{bmatrix} \begin{Bmatrix} \ddot{\mathbf{q}} \\ \boldsymbol{\lambda} \end{Bmatrix} = \begin{Bmatrix} \mathbf{g} \\ \boldsymbol{\gamma} \end{Bmatrix} \qquad (4)$$

where $\boldsymbol{\lambda}$ is the vector of Lagrange multipliers, which physically are related to the joint reaction forces. The reaction forces, owing to the kinematic joints are expressed as [18],

$$\mathbf{g}^{(c)} = -\mathbf{\Phi}_{\mathbf{q}}^{T}\boldsymbol{\lambda} \qquad (5)$$

Equation (4) is a differential-algebraic equation that has to be solved and the resulting accelerations integrated in time. However, they do not use explicitly the position and velocity constraint equations allowing for a drift in the system constraints to develop. In order to keep under control such constraint violation during the numerical integration the Baumgarte stabilization technique is employed, and Eq. (4) modified as

$$\begin{bmatrix} \mathbf{M} & \mathbf{\Phi}_{\mathbf{q}}^{T} \\ \mathbf{\Phi}_{\mathbf{q}} & \mathbf{0} \end{bmatrix} \begin{Bmatrix} \ddot{\mathbf{q}} \\ \boldsymbol{\lambda} \end{Bmatrix} = \begin{Bmatrix} \mathbf{g} \\ \boldsymbol{\gamma} - 2\alpha\dot{\mathbf{\Phi}} - \beta^{2}\mathbf{\Phi} \end{Bmatrix} \qquad (6)$$

where α and β are prescribed positive constants that represent the feedback control parameters for the velocities and positions constraint violations [14,15].

According to this formulation, the dynamic response of multibody systems involves the evaluation of the vectors $\mathbf{g}$ and $\boldsymbol{\gamma}$, for each time step. Then, Eq. (6) is solved for the system accelerations $\ddot{\mathbf{q}}$. These accelerations together with the velocities $\dot{\mathbf{q}}$ are integrated in order to obtain the new velocities $\dot{\mathbf{q}}$ and positions $\mathbf{q}$ for the next time step. This process is repeated until the complete description of system motion is performed. Figure 1 shows the standard flowchart for the dynamic solution of the differential-algebraic equations of motion (4).

3. MATHEMATICAL MODEL FOR TRANSLATIONAL CLEARANCE JOINTS

The purpose of this section is to present a mathematical model for translational joints with clearance in multibody systems. Figure 2 shows a planar translational joint with clearance. The clearance c is defined as the difference between the distance of the guide and the slider surfaces. Other important geometric characteristics of the translational clearance joint are the length of the slider L, the slider width W, and the total distance between the guide surfaces H. Mathematically, clearance can be expressed as,

$$c = \frac{H - W}{2} \qquad (7)$$

In an ideal translational joint the two bodies, slider and guide, translate with respect to each other parallel to the line of translation, so that, there is neither rotation between the bodies nor relative translation motion in the direction perpendicular to the line of translation. Therefore, an ideal translational joint reduces the number of degrees of freedom of the system by two. The existence of a clearance in a translational joint eliminates the two kinematic constraints and introduces two extra degrees of freedom. Hence, the slider can freely move inside the guide limits. When the slider reaches the guide surfaces an impact occurs and the dynamic response of the joint is modeled by contact forces. These contact forces are evaluated according to a continuous contact force law together with the dissipative friction force law. Then these forces are introduced into the system's equations of motion as external generalized forces. Although a translational clearance joint does not constraint any degree of freedom from the mechanical system as an ideal joint, it imposes some restrictions on the slider motion inside the guide. Thus, while a perfect joint in multibody system is achieved by kinematic constraints, a clearance joint is obtained by a force constraint.

There are several possible configurations for the relative position between the slider and guide, as illustrated in Fig. 3. These different configurations are:

- There is no contact between the two elements, i.e., the slider is in free flight motion inside the guide and, consequently, there is no reaction force at the joint;
- One corner of the slider in contact with the guide surface;

- Two adjacent slider corners are in contact with the guide surface, which corresponds to have a face of slider is in contact with the guide surface;
- Two opposite slider corners are in contact with the guide surface.

The conditions for switching from one case to another one depend on the system dynamics configuration. For the three last cases, the contact forces are evaluated according to a continuous contact force model.

In order for the translational clearance joints to be used in the multibody system models it is required that a mathematical model is developed. Figure 4 shows a representation of a translation joint with clearance that connects bodies *i* and *j*. The slider is body *i* whereas the guide is part of body *j*. The center of mass of bodies *i* and *j* are O_i and O_j, respectively. Local coordinate systems are attached at the center of mass of each body, while XY coordinate frame represents the global coordinate system. Let points *P*, *Q*, *S* and *R* in the guide surfaces indicate the geometric limits inside which contact may occur. Points A_i, B_i, C_i and D_i indicate the four slider corners, and A_j, B_j, C_j and D_j are the points on the guide surfaces that are closer to the respective points in body *j*. As the formulation for all the slider corners is similar, in what follows, only the slider corner *A* is used to describe the mathematical model.

Let vector $\mathbf{t}$, directed along the guide surface from point *P* to point *Q* in body *j*, be written in terms of the body fixed coordinates as

$$\mathbf{t}'_j = \mathbf{s}'^{Q}_j - \mathbf{s}'^{P}_j \qquad (8)$$

Note that if expressed in the inertia frame the tangent vector $\mathbf{t}=\mathbf{A}_j\mathbf{t}'$, where $\mathbf{A}_j$ is the transformation matrix from body *j* frame to the inertial frame.

Let the position vector for any given point *G* of a body *k* be described with respect to inertial reference frame as

$$\mathbf{r}^G_k = \mathbf{r}_k + \mathbf{A}_k\mathbf{s}'^G_k, \quad (k=i,j) \qquad (9)$$

where $\mathbf{s}'^G_k$ is the position of point *G* in body *k* expressed in body fixed coordinates. The position of point A_j, belonging to the segment $\overline{PQ}$ of the guide, closest to point A_i located in the corner of the slider, is given as

$$\mathbf{r}_j^A = \mathbf{r}_j^P + \left[\mathbf{t}^T \left(\mathbf{r}_i^A - \mathbf{r}_j^P\right)\right]\mathbf{t} \qquad (10)$$

The vector that connects the slider corner A_i to point A_j on the guide surface is defined as

$$\boldsymbol{\delta} = \mathbf{r}_j^A - \mathbf{r}_i^A \qquad (11)$$

Note that vector $\boldsymbol{\delta}$ has the same direction as the normal **n** to the guide surface. However, regardless of this identity, let the normal vector **n** be defined as perpendicular to the tangent vector **t**, which for two-dimensional cases is

$$\mathbf{n} = \begin{bmatrix} t_{(y)} & -t_{(x)} \end{bmatrix}^T \qquad (12)$$

where $t_{(x)}$ and $t_{(y)}$ are the inertial components of the tangential vector projected onto the X and Y directions, respectively.

Figure 5 shows the slider and guide in two different scenarios, namely in a non contact situation and in the case of penetration between the slider and guide surface. For the contact case, the vectors $\boldsymbol{\delta}$ and **n** are parallel but oriented in opposite directions, i.e. their scalar product is negative. Thus, the condition for penetration between the slider and guide is expressed as

$$\mathbf{n}^T\boldsymbol{\delta} < 0 \qquad (13)$$

The magnitude of the penetration depth for point A_i is evaluated as

$$\delta = \sqrt{\boldsymbol{\delta}^T\boldsymbol{\delta}} \qquad (14)$$

The impact velocity, required for the evaluation of the contact force, is obtained by differentiating Eq. (11) with respect to time yielding

$$\dot{\boldsymbol{\delta}} = \dot{\mathbf{r}}_j + \dot{\mathbf{A}}_j\mathbf{s}'^A_j - \dot{\mathbf{r}}_i - \dot{\mathbf{A}}_i\mathbf{s}'^A_i \qquad (15)$$

The evaluation of the contact forces is made in next sections. However, note that the points of application of such forces in bodies *i* and *j* are points A_i and A_j, respectively.

4. CONTACT FORCE MODEL

In dealing with translational clearance joints, it is essential to define how the slider and guide surfaces contact each other and, consequently, what is the most adequate contact force model. In a general way, the contact-impact force models can include three different components: the elastic force, the damping force and the friction force [19]. Furthermore, the contact force model is expected to contribute to the stable integration of the equations of motion of the multibody system. In this work different contact force models based on penalization methods are presented and applied to a demonstrative problem with a translational clearance joint.

4.1. Elastic Contact Force

The elastic force developed in the contact collision between the slider and guide surfaces can be modeled by applying the Hertz contact law, which is based on the elasticity theory [20]. The Hertz contact model represents the contact force as a nonlinear function of the penetration. This is expressed as [21]

$$f_N = K\delta^n \qquad (16)$$

in which K is the generalized stiffness constant and δ is the relative penetration depth. The exponent n is equal to 1.5 for metals. Hunt and Crossley [22] suggested the use of the contact law given by Eq. (16) with a power exponent $1<n<1.5$. The generalized stiffness depends on the materials and on the geometry of the contacting bodies. For instance, for the contact between a spherical body i and a plane surface the generalized stiffness constant depends on the radius of the sphere and the materials properties, and is expressed by [23]

$$K = \frac{4}{3(\sigma_i + \sigma_j)}\sqrt{R_i} \qquad (17)$$

where R_i is the radius of curvature of the sphere and σ_i and σ_j are given by

$$\sigma_k = \frac{1-\nu_k^2}{E_k}, \quad (k=i,j) \qquad (18)$$

variables ν_k and E_k are, respectively, the Poisson's ratio and the Young's modulus associated with the material of each body.

For contact between square plane surfaces a linear elastic force model is expressed as [24]

$$f_N = K\delta \qquad (19)$$

where the stiffness parameter K is given by

$$K = \frac{a}{0.475(\sigma_i + \sigma_j)} \qquad (20)$$

the area of contact is a square with a side of $2a$, and the variables σ_i and σ_j are given by Eq. (18). The contact force law given by Eq. (19) is linear, which seems acceptable since there is no geometric nonlinearity due to the curvature of the bodies.

The continuous contact force model described here uses, for each contact conditions, fixed values for the proportional coefficient K that appears in equations (16) through (20). However, it should be emphasized that during a general contact problem the shape of the contacting surfaces may change and that a particular expression for K, regardless of being equation (17) or (20) are not valid anymore, in a strict sense. For instance, when considering a single corner contact as implied by figure 6(b) the motion of the system may be such that its evolution leads to a two surface contact as depicted by figure 6(a) without any contact lost in between those two instants in time. Clearly the need for a transition model for the parameter K is required, provided that it would not violate the basic assumptions of the Hertz elastic contact theory implied in equation (16). Such model is not presented here but may be required to complement with more realism the applications of the methodologies proposed here.

4.2. Damping Force

Hunt and Crossley [22] proposed a nonlinear viscous-elastic model to represent the damping force, which simulates the energy transferred during the impact process. Based on the work of Hunt and Crossley, Lankarani and Nikravesh [12] presented a continuous contact force model in which a hysteretic damping factor is incorporated in order to account for the energy dissipation during the contact. This contact force model is expressed as

$$f_N = K\delta^n \left[1 + \frac{3(1-e^2)}{4} \frac{\dot{\delta}}{\dot{\delta}^{(-)}} \right] \qquad (21)$$

where the generalized stiffness parameter K is evaluated by equations such as (17) and (18), e is the restitution coefficient, $\dot{\delta}$ is the relative penetration velocity and $\dot{\delta}^{(-)}$ is the initial impact velocity. Equation (21) is used to simulate the impact because it accounts for energy dissipation and exhibits good numerical stability at low impact velocities [25].

When two adjacent slider corners contact with the guide surface, the resulting contact force is applied at the geometric center of the penetration area, denoted as GC in Fig. 6(a), and the contact force model given by Eq. (19) is used. Otherwise, when one or two opposite slider corners contact the guide surface, the contact area is too small. Thus, the contact is assumed to be between a spherical surface and a plane surface, allowing for the contact model given by Eq. (21) to be applied. In order to evaluate the equivalent stiffness a small curvature radius R is assumed on the contact corner, represented in Fig. 6(b).

4.3. Friction Force

In a multibody system a friction force is likely to appear in joints where the contacting surfaces have a relative sliding motion. The Coulomb law [26] of sliding friction can represent the most fundamental and simplest model of friction between dry contacting surfaces. However, the implementation of the standard Coulomb friction model in a general-purpose program can lead to numerical difficulties. In order to avoid such difficulties, a modified Coulomb law is used [13]

$$f_T = -c_f c_d f_N \frac{\mathbf{v}_T}{\|\mathbf{v}_T\|} \qquad (22)$$

where c_f is the friction coefficient, f_N is the normal force, $\mathbf{v}_T$ is the relative tangential velocity and c_d is a dynamic correction coefficient, which is expressed as [13]

$$c_d = \begin{cases} 0 & \text{if} \quad v_T \le v_0 \\ \dfrac{v_T - v_0}{v_1 - v_0} & \text{if} \quad v_0 \le v_T \le v_1 \\ 1 & \text{if} \quad v_T \ge v_1 \end{cases} \qquad (23)$$

where v_0 and v_1 are given positive tolerances for the velocity. The dynamic correction factor c_d prevents that the friction force changes direction in the presence of almost null values of the tangential velocity, which would be perceived by the integration algorithm as a dynamic response with high frequency contents, forcing it to reduce the time step size. The modified friction model represented by Eq. (22) does not account for other tribology phenomena like adherence between the sliding contact surfaces.

4.4. Force Resultants and Equivalent Moments on the Rigid Bodies

As seen before, when the contact between the slider and the guide surface takes place, normal and tangential forces act at the contact point or surface. These forces need to be transferred to the center of mass of each body. Referring to Fig. 7, the equivalent system of forces and moments acting on the center of mass of body *i* is expressed by

$$\mathbf{f}_i = \mathbf{f}_N + \mathbf{f}_T \qquad (24)$$

$$\mathbf{m}_i = -(y_i^Q - y_i)\mathbf{f}_i^x + (x_i^Q - x_i)\mathbf{f}_i^y \qquad (25)$$

The forces and moments corresponding to the body *j* are written as

$$\mathbf{f}_\mathrm{j} = -\mathbf{f}_\mathrm{i} \qquad (26)$$

$$\mathbf{m}_j = (x_j^Q - x_j)\mathbf{f}_j^y - (y_j^Q - y_j)\mathbf{f}_j^x \qquad (27)$$

5. NUMERICAL RESULTS AND DISCUSSION

In order to examine the effectiveness of the formulation developed for the translational clearance joint, the planar slider-crank mechanism is considered as a numerical example. The slider-crank mechanism is made up of four rigid bodies connected by three ideal revolute joints and one translational joint with clearance, composed by a guide and a slider as shown in Fig. 8. This joint has a finite clearance constant along the length of the slider. The dimensions and inertia properties of each body are given in Table 1 [27].

It is assumed that the crank is driven with a constant angular velocity equal to 5000 rpm maintained by a kinematic driving constraint. Initially, the slider is at the same distance from the upper and lower guide surfaces. Furthermore, the initial simulation configuration of the slider-crank mechanism corresponds to the top dead end. The impact between the slider and guide surfaces is frictionless and modeled by the Lankarani and Nikravesh contact force model expressed by Eq. (21). For convenience, a small radius of curvature at each slider corner is assumed. Table 2 shows the dynamic parameters used in the simulations.

Body No	Length [m]	Mass [Kg]	Moment of inertia [Kgm^2]
2	0.05	0.30	0.00010
3	0.12	0.21	0.00025
4	-	0.14	0.00010

Table 1. Dimensions and inertia properties of the slider-crank mechanism.

Clearance size	0.5 mm	Young's modulus	207 GPa
Slider length	50.0 mm	Poisson's ratio	0.3
Slider width	50.0 mm	Baumgarte - α	5
Slider thickness	50.0 mm	Baumgarte - β	5
Corner curvature radius	1.0 mm	Integration step size	0.00001 s
Restitution coefficient	0.9	Integration tolerance	0.000001

Table 2. Simulation parameters used in the dynamic simulation of the slider-crank mechanism.

The dynamic performance of the slider-crank mechanism simulation is quantified by plotting the values of the slider velocity and acceleration, and the moment acting on the crank. Additionally, the slider trajectories inside the guide are plotted in a non-dimensional form. Results for to two full crank rotations are given in Fig. 9.

The observation of the slider velocity and acceleration curves, presented in Fig. 9(a) and 9(b) shows very clearly the influence of the translational clearance joint in the kinematics of the slider. The slider velocity diagram is very smooth and close to ideal joint simulation. The smooth changes in the velocity also indicate that the slider and guide surfaces are in permanent contact for long periods. Some sudden changes in the velocity are due to the impacts between the slider and guide surfaces. These impacts are better visible in the acceleration diagram by high peak values. Since the bodies of the slider-crank mechanism are rigid, the impact forces are propagated from the slider to the crank, leading to visible high peaks on the crank diagram moment shown in Fig. 9(c).

The dimensionless slider trajectories are shown in Fig. 9(d), where the different types of motion between the slider and guide observed are associated with the different guide-slider configurations, i.e., no contact, contact-impact followed by rebound and permanent contact. The dimensionless X-slider motion varies from 0 to 1, which corresponds to the low and top dead ends, respectively. When the dimensionless Y-slider motion is higher than 0.5, corresponds to the case in which the slider and the upper guide surface are in a contact situation, whereas, when the dimensionless Y-slider motion is lower than -0.5, corresponds to the case in which the slider and lower guide surface are in contact. The horizontal lines in the slider path diagrams represent geometric limit for contact situation between the slider and guides surfaces.

In order to understand the influence of the clearance size in the dynamic behavior of the slider-crank mechanism, the driving crank moment is plotted in Fig. 10. In addition to the crank moment, the slider trajectories and the Poincaré maps are presented in Fig. 11 and 12, respectively. Clearance values of 0.5 mm, 0.2 mm, 0.1 mm and 0.01 mm are analyzed.

By observing Fig. 10 it is evident that when the clearance size is small the crank moment peaks are lower and the dynamic response tends to be closer to the ideal translation joint case. This suggests that the periods of permanent contact between the slider and guide surfaces are longer and, hence, the slider and guide experiment fewer impacts. This observation can be confirmed by the slider trajectories and Poincaré maps provided in figures 11 and 12 respectively. In fact, when the clearance size is reduced, the system response changes from chaotic or nonlinear, as displayed in Fig. 12(a), to periodic or regular, as observed in Fig. 12(d). This feature

can be useful in calculations of the acceptable range for clearance for any type of construction where this type of joints is applied.

The influence of employing different contact force models on the global slider-crank behavior is also analyzed in this work. Figures 13 and 14 show the contact force and driving crank moment for the contact force models given by Eqs. (20) and (18), respectively. In the case of the linear contact model for two plane surfaces, the average penetration is used to evaluate the magnitude of the contact force. This force is then applied at the geometric center of the penetration area, as schematically shown in Fig. 6(a).

By observing Figs. 13 and 14 it is visible that the linear force model produces higher peaks when compared to the case of nonlinear contact force model. Both the joint contact force and the driving crank moment peaks are about ten times higher in the linear force model than the peaks observed for when the nonlinear contact law is applied. This can be explained by the fact of the linear model does not account for the energy dissipation during the impact process whereas the continuous contact force model besides being based on the Hertz contact law also represents the energy dissipation.

At this point it must be emphasized that the use of the driving constraint, which ensures that the crank rotates with constant angular velocity, is a very simplified model of a realistic driving system. In fact, provided that there are no kinematic jamming conditions in the mechanism, i.e., that the mechanism does not lock due to its kinematic constraints, the driving constraint implied in equation (5) is always able to force the crank to move with the same angular velocity because it is always able to provide any power required to oppose resisting forces in the mechanism. Certainly that other descriptions of the driving mechanism not based on the use of kinematic driving constraints would be sensitive to the raise in forces opposing the slider motion, such as those arising from normal contact and friction. In this case it can be expected that the peaks in the contact forces, and also in the accelerations, are lower than what is observed for the ideal kinematically driven crank. Also, the existence of friction in the model would lower the size of the force and acceleration peaks and lead to more realistic values for the system response. However, none of these features has any relation with the detection of contact of the prismatic clearance joint that is the objective of the methodology described in this work.

6. CONCLUDING REMARKS

A methodology for translational joints with clearance in rigid multibody systems was presented and discussed in the present work. The slider and the guide elements that constitute a translational clearance joint are modeled as two colliding bodies being the dynamics of the joint controlled by the contact-impact forces. The equations of motion that govern the dynamic response of the general multibody systems incorporate the impact forces due to the collisions of the bodies that constitute the translational clearance joints. A continuous contact force model provides the intra-joint impact forces that develop during the normal operations of the mechanisms.

The planar slider-crank mechanism with a translational clearance joint was used as a numerical example to illustrate the methodology proposed. In general, the dynamic response of the slider-crank mechanism presents some peaks due to the impact between the slider and guide, namely in what concerns to the accelerations and crank driving moments. It was observed that all curves for the kinematic and dynamic variables are similar to those obtained with ideal joints, with the exception of the peaks especially visible for the forces and accelerations. These peaks have been clearly related to the existence of the clearances and to their magnitude.

The relative motion between the guide and slider showed a very high nonlinearity or even chaotic behavior when a translational clearance is included. When the clearance size is reduced the systems response becomes closer to the case for ideal joints. Furthermore, the dynamic behavior of the slider-crank model tends to be periodic or regular. This feature can be a useful tool in calculations of the acceptable range for clearance during the design of a multibody system.

ACKNOWLEDGMENTS

The research work presented in this paper was supported by *Fundação para a Ciência e a Tecnologia* and partially financed by *Fundo Comunitário Europeu FEDER* under project POCTI/2001/EME/38281, entitled 'Dynamic of Mechanical Systems with Joint Clearances and Imperfections'.

REFERENCES

[1] Haines, R.S., 1980, "Survey: 2-Dimensional Motion and Impact at Revolute Joints", Mechanism and Machine Theory, **15**, pp. 361-370.

[2] Bengisu, M.T., Hidayetoglu, T. and Akay, A., 1986, "A Theoretical and Experimental Investigation of Contact Loss in the Clearances of a Four-Bar Mechanism", Journal of Mechanisms, Transmissions, and Automation Design, **108**, pp. 237-244.

[3] Ravn, P., 1998, "A Continuous Analysis Method for Planar Multibody Systems with Joint Clearance", Multibody System Dynamics, **2**, pp. 1-24.

[4] Flores, P., Ambrósio, J. and Claro, J.C.P., 2004, "Dynamic Analysis for Planar Multibody Mechanical Systems with Lubricated Joints", Multibody System Dynamics, **12**, pp. 47-74.

[5] Liu, C., Zhang, K. and Yang, L., 2006, "Normal Force-Displacement Relationship of Spherical Joints With Clearances", Journal of Computational and Nonlinear Dynamics, **1**(2), pp 160-167.

[6] Flores, P., Ambrósio, J., Claro, J.C.P. and Lankarani, H.M., 2006, "Dynamics of Multibody Systems with Spherical Clearance Joints", Journal of Computational and Nonlinear Dynamics, **1**(3), pp 240-247.

[7] Bauchau, O.A. and Rodriguez, J., 2002, "Modelling of Joints with Clearance in Flexible Multibody Systems", International Journal of Solids and Structures, **39**, pp. 41-63.

[8] Flores, P., Lankarani, H.M., Ambrósio, J. and Claro, J.C.P., 2004, "Modeling lubricated revolute joints in multibody mechanical systems", Proceedings of the Institution of Mechanical Engineers, Part-K Journal of Multi-body Dynamics, **218**, pp. 183-190.

[9] Wilson, R. and Fawcett, J.N., 1974, "Dynamics of the Slider-Crank Mechanism with Clearance in the Sliding Bearing", Mechanism and Machine Theory, **9**, pp. 61-80.

[10] Farahanchi, F. and Shaw, S., 1994, "Chaotic and Periodic Dynamics of a Slider-Crank Mechanism with Slider Clearance", Journal of Sound and Vibration, **177**(3), pp. 307-324.

[11] Thümmel, T. and Funk, K., 1999, "Multibody Modeling of Linkage Mechanisms including Friction, Clearance and Impact", Proceedings of 10th World Congress on TMM in Oulu, Finland, Oulu University Press, Vol. 4, pp. 1375-1386 (1999).

[12] Lankarani, H.M., and Nikravesh, P.E., 1990, "A Contact Force Model With Hysteresis Damping for Impact Analysis of Multibody Systems", Journal of Mechanical Design, **112**, pp. 369-376.

[13] Ambrósio, J.A.C., 2002, "Impact of Rigid and Flexible Multibody Systems: Deformation Description and Contact Models", *Virtual Nonlinear Multibody Systems, NATO, Advanced Study Institute*, (edited by W. Schiehlen and M. Valásek), Vol. II, pp. 15-33.

[14] Nikravesh, P.E., 1988, *Computer-Aided Analysis of Mechanical Systems*, Prentice-Hall, Englewood Cliffs, New Jersey.

[15] Baumgarte, J., 1972, "Stabilization of Constraints and Integrals of Motion in Dynamical Systems", Computer Methods in Applied Mechanics and Engineering, **1**, pp. 1-16.

[16] Shampine, L., and Gordon, M., 1975, *Computer Solution of Ordinary Differential Equations: The Initial Value Problem*. Freeman, San Francisco, California.

[17] Gear, C.W., 1981, "Numerical Solution of Differential-Algebraic Equations", IEEE Transactions on Circuit Theory, Vol. CT-18, pp. 89-95.

[18] Garcia de Jalon, J. and Bayo, E., 1994, *Kinematic and Dynamic Simulations of Multibody Systems*, Springer-Verlag, New York.

[19] Flores, P., Ambrósio, J., Claro, J.C.P. and Lankarani, H.M., 2006, "Influence of the contact-impact force model on the dynamic response of multibody systems", Proceedings of the Institution of Mechanical Engineers, Part-K Journal of Multi-body Dynamics, **220**, pp. 21-34.

[20] Timoshenko, S.P. and Goodier, J.N., 1970, *Theory of Elasticity*, McGraw Hill, New York.

[21] Hertz, H., 1896, *On the contact of solids - On the contact of rigid elastic solids and on hardness*, (Translated by D. E. Jones and G. A. Schott), Miscellaneous Papers, MacMillan and Co. Ltd., London, 146-183.

[22] Hunt, K.H. and Crossley, F.R., 1975, "Coefficient of Restitution Interpreted as Damping in Vibroimpact", Journal of Applied Mechanics, **7**, pp. 440-445.

[23] Goldsmith, W., 1960, *Impact - The Theory and Physical Behaviour of Colliding Solids*, Edward Arnold Ltd, London.

[24] Lankarani, H.M., 1988, *Canonical Equations of Motion and Estimation of Parameters in the Analysis of Impact Problems*, Ph.D. Dissertation, University of Arizona, Tucson, Arizona, USA.

[25] Love, A., 1944, *A Treatise on the Mathematical Theory of Elasticity*, Fourth edition, Dover Publications, New York.

[26] Greenwood, D.T., 1965, *Principles of Dynamics*, Prentice Hall, Englewood Cliffs, New Jersey.

[27] Flores, P., 2005, *Dynamic Analysis of Mechanical Systems with Imperfect Kinematic Joints*, PhD Dissertation, University of Minho, Guimarães, Portugal.

LIST OF FIGURES

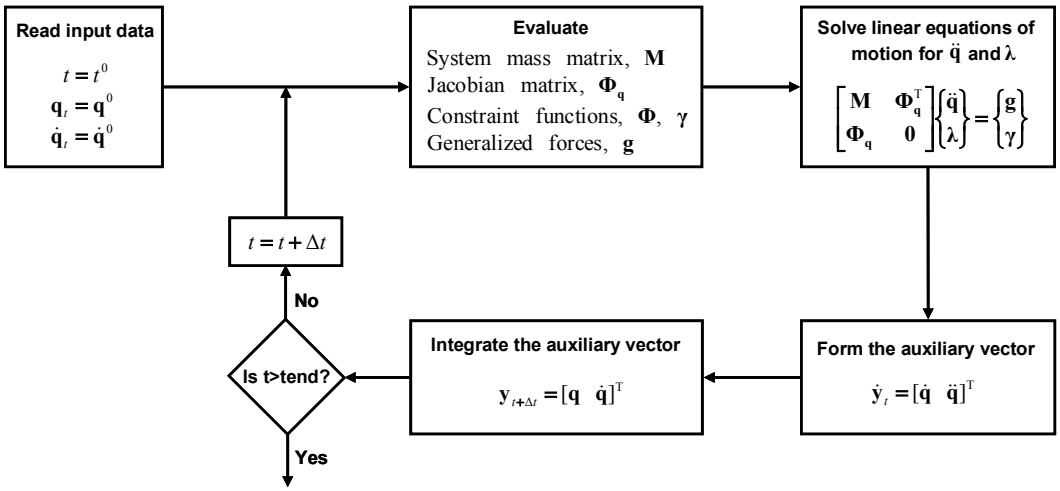

Fig. 1: Standard procedure to solve the differential-algebraic equations of motion of a multibody system.

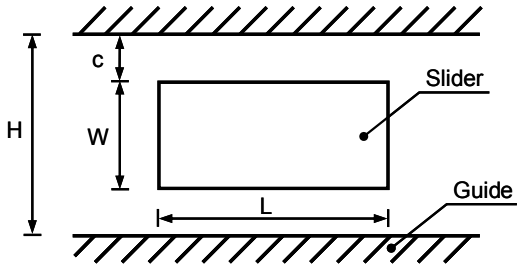

Fig. 2: Planar translational joint with clearance constituted by a slider and its guide.

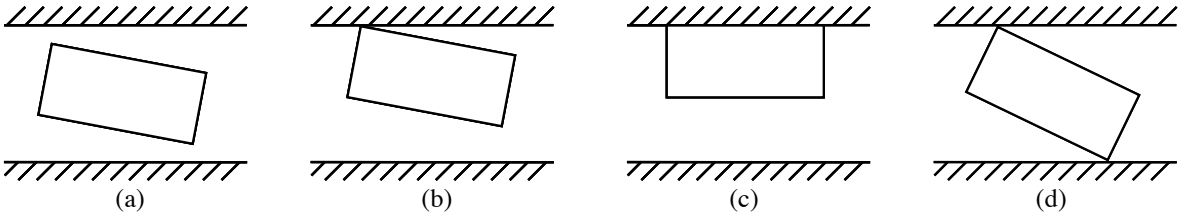

Fig. 3: Different scenarios for the slider motion inside the guide: (a) no contact; (b) one corner in contact with the guide; (c) two adjacent corners in contact with guide; (d) two opposite corners in contact with guide.

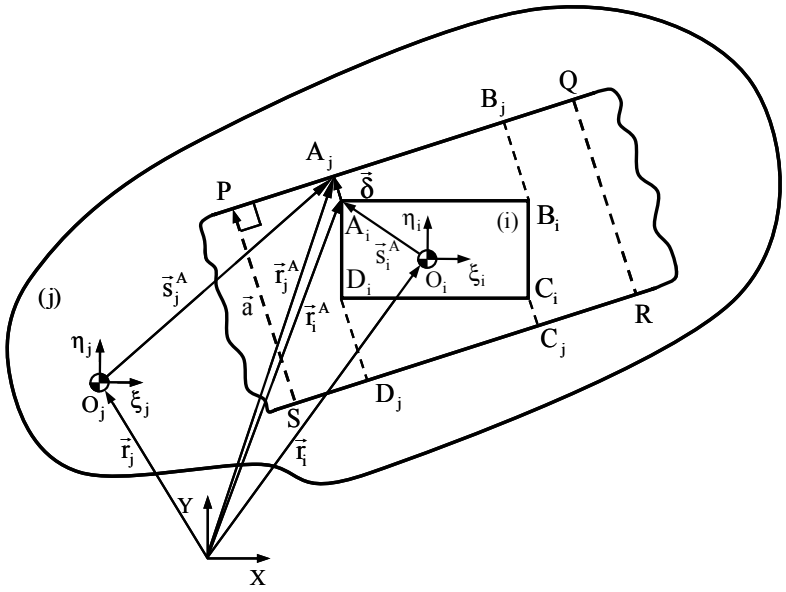

Fig. 4: Generic translational clearance joint in a multibody system.

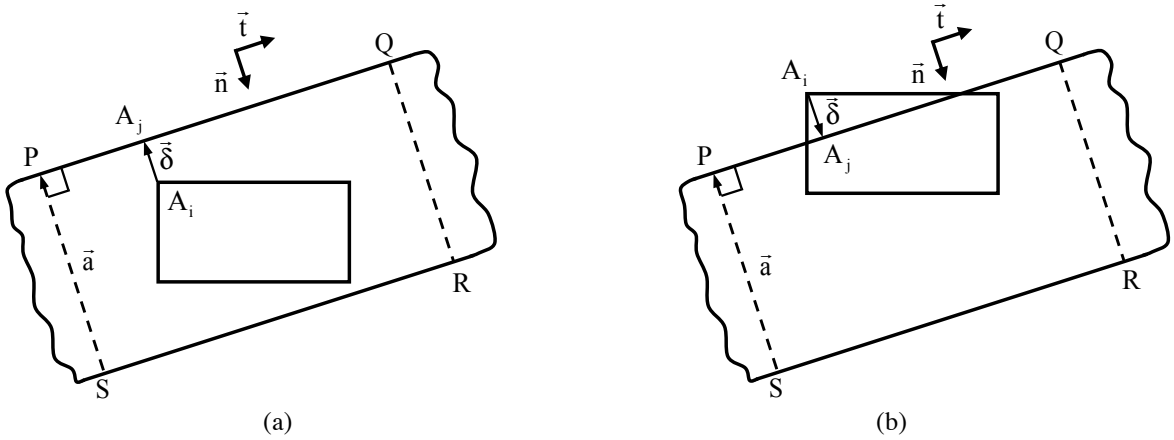

Fig. 5: (a) Non contact situation; (b) Penetration between the slider corner *A* and guide surface.

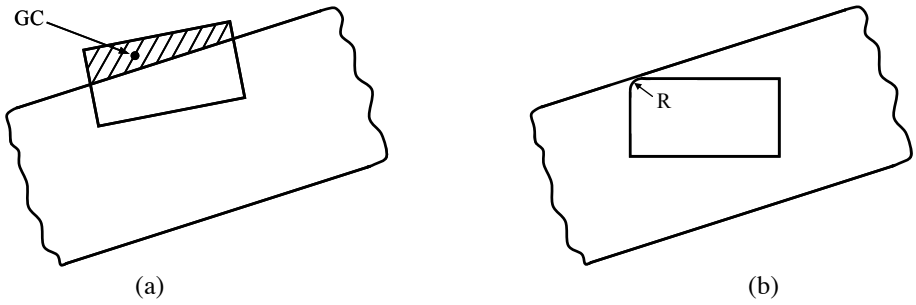

Fig. 6: (a) Contact between two plane surfaces; (b) Contact between a spherical surface and a plane.

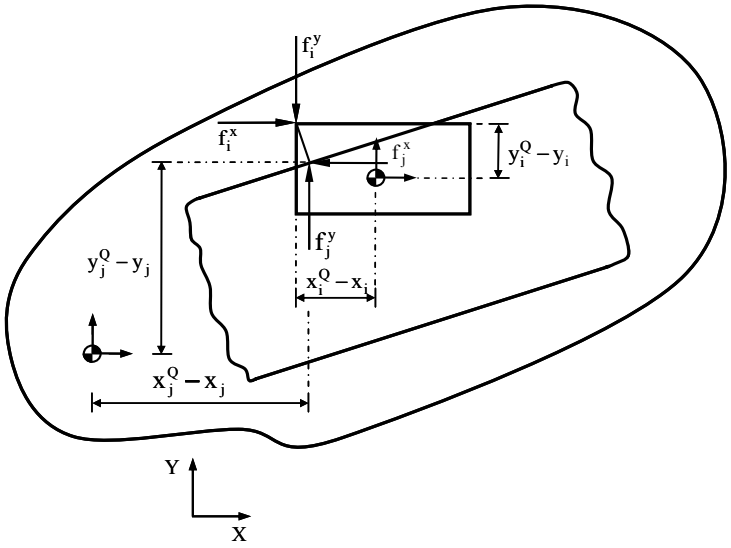

Fig. 7: Contact forces defined at the points of contact between the slider and guide.

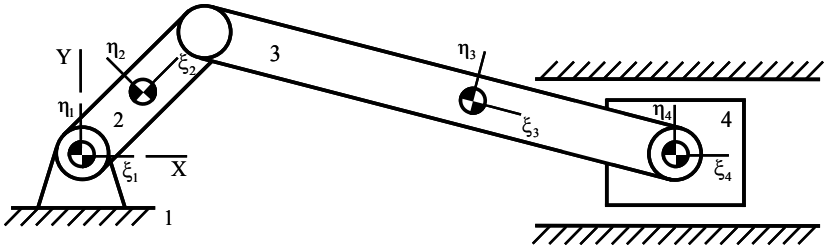

Fig. 8: Slider-crank mechanism with a translational clearance joint.

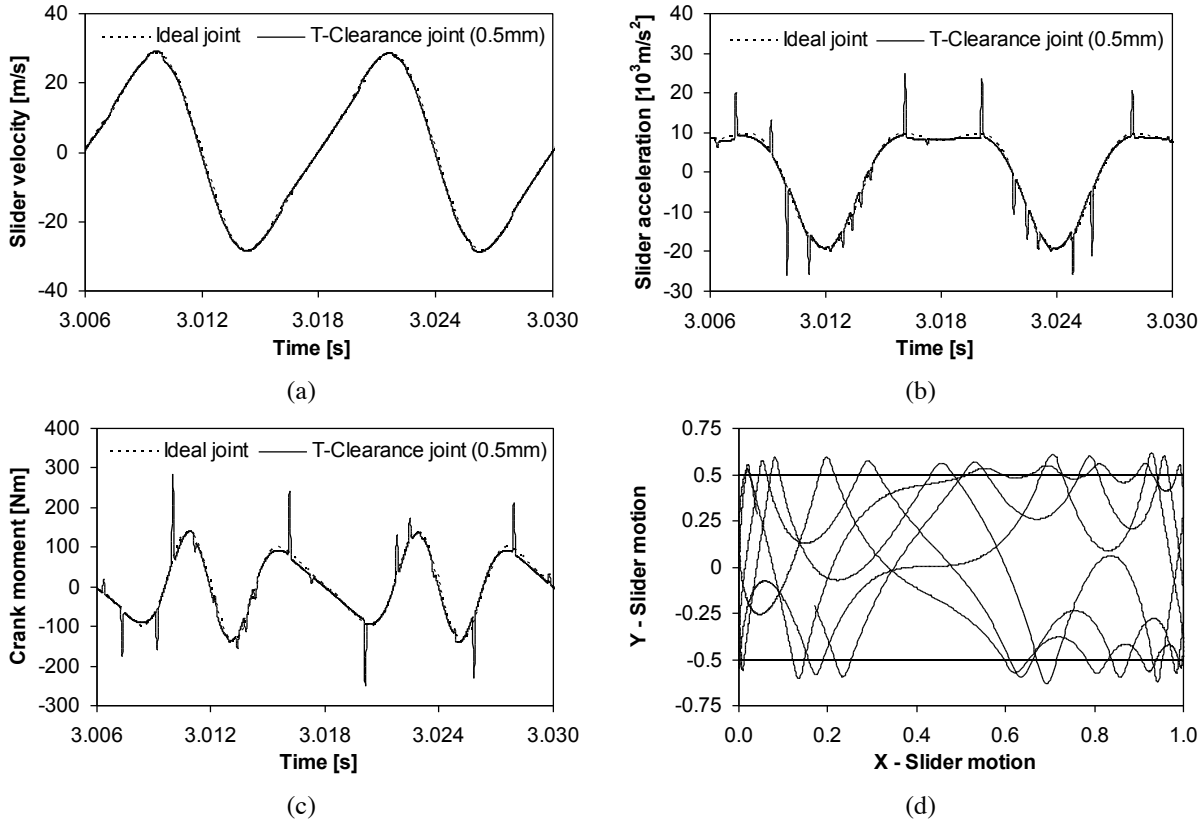

Fig. 9: (a) Slider velocity; (b) Slider acceleration; (c) Crank moment; (d) Dimensionless slider trajectories inside the guide.

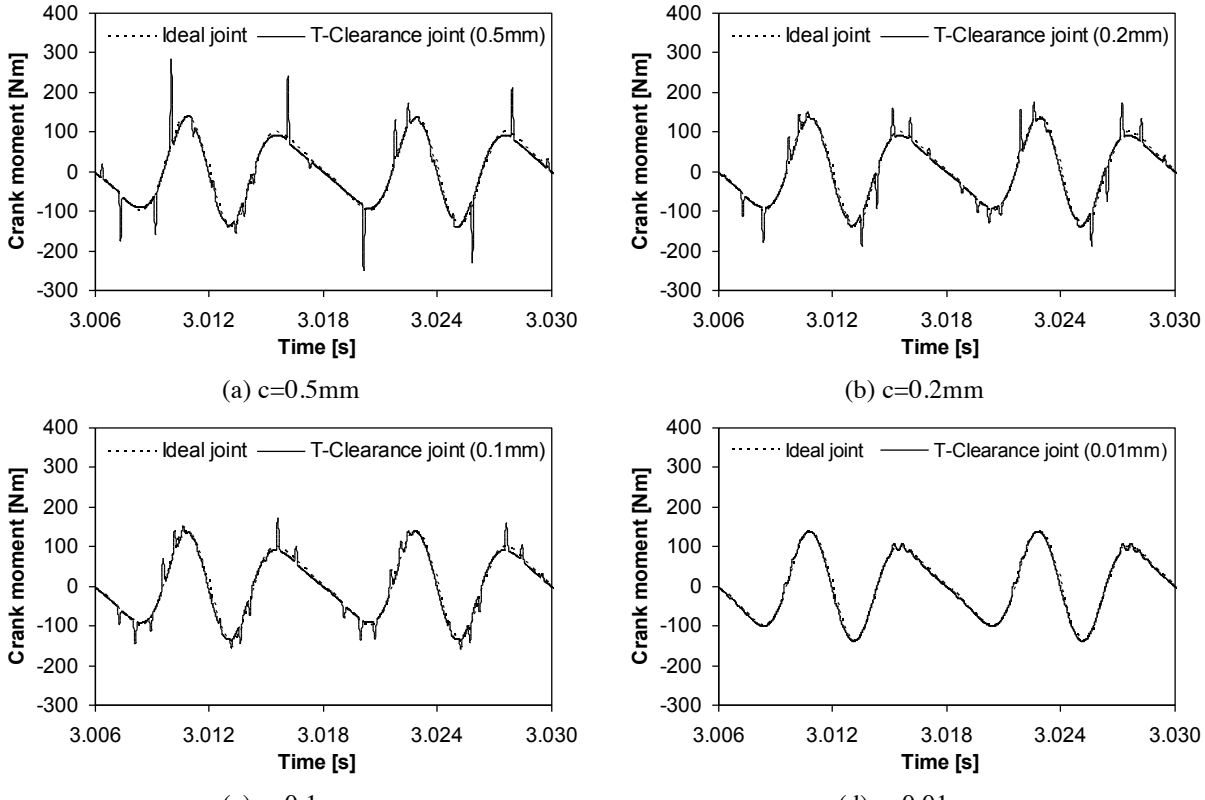

Fig. 10: Driving crank moment for different clearance sizes in the translational clearance joint.

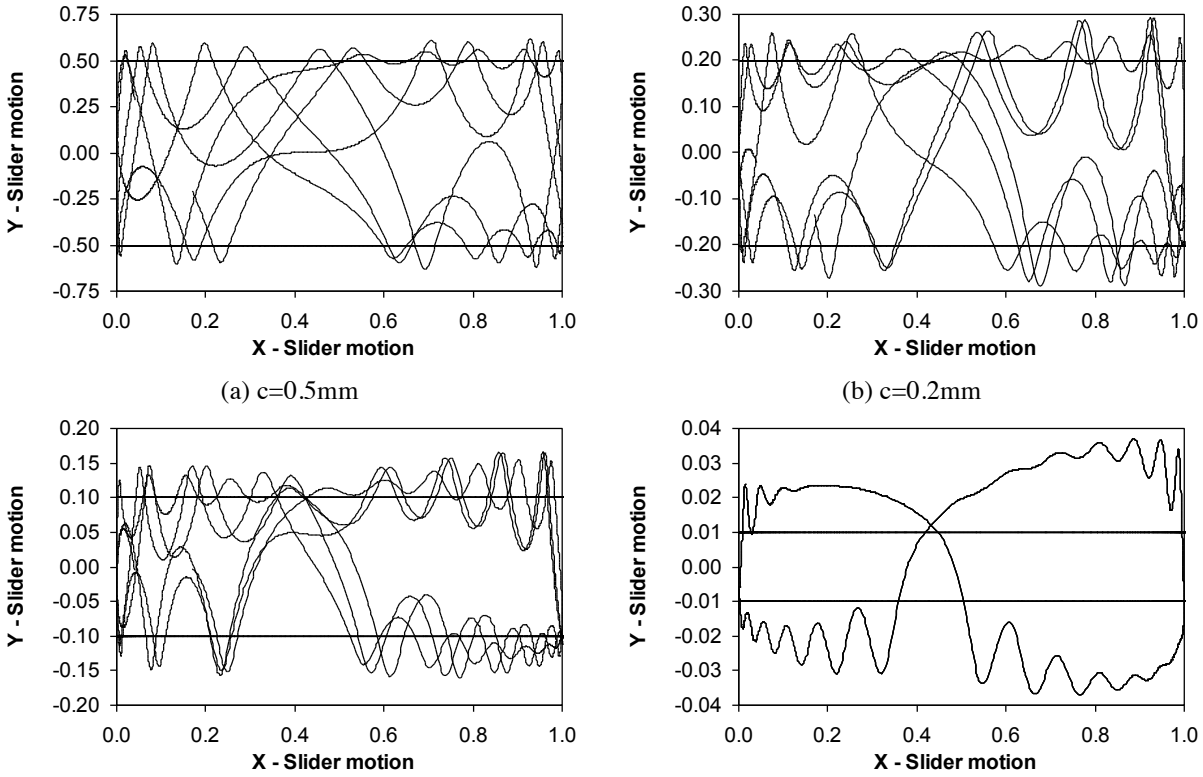

(a) c=0.5mm (b) c=0.2mm

(c) c=0.1mm (d) c=0.01mm

Fig. 11: Dimensionless slider path for different clearance sizes in the translational clearance joint.

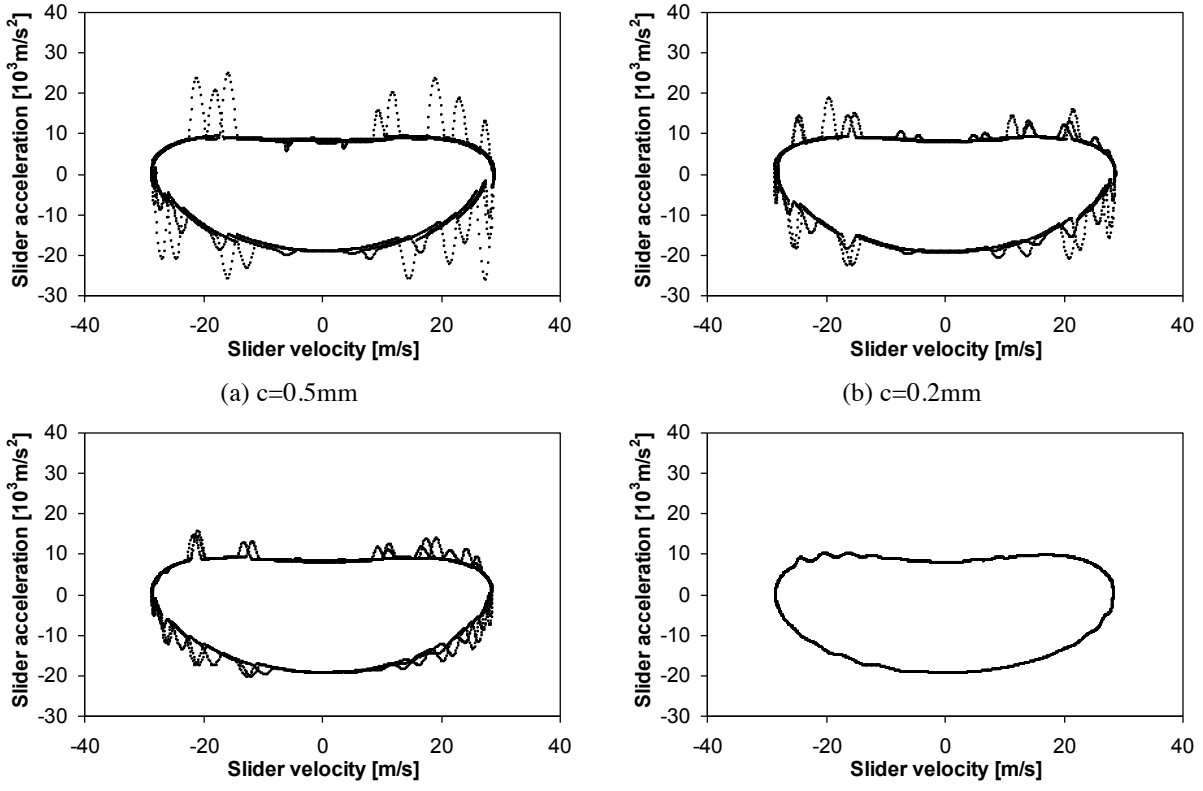

(a) c=0.5mm (b) c=0.2mm

(c) c=0.1mm (d) c=0.01mm

Fig. 12: Poincaré maps for different clearance sizes in the translational clearance joint.

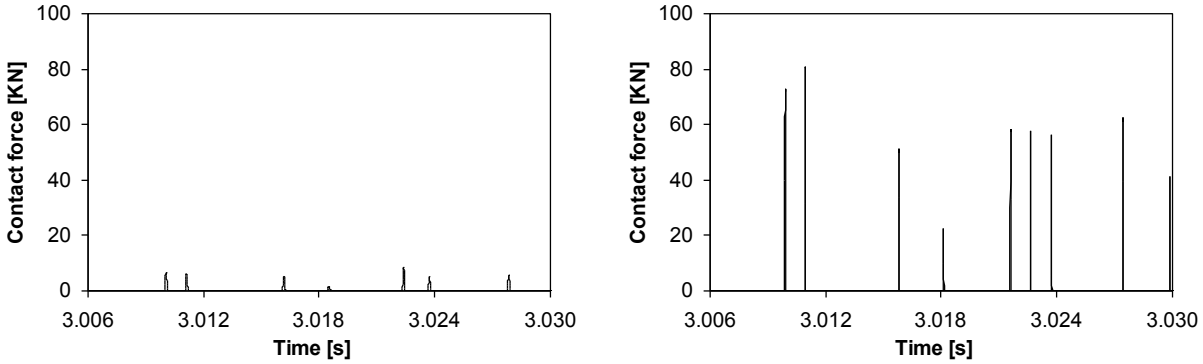

(a) (b)

Fig. 13: Contact force between the slider and guide surface: (a) Lankarani and Nikravesh model given by Eq. (20); (b) Linear contact model for two plane surfaces expressed by Eq. (18).

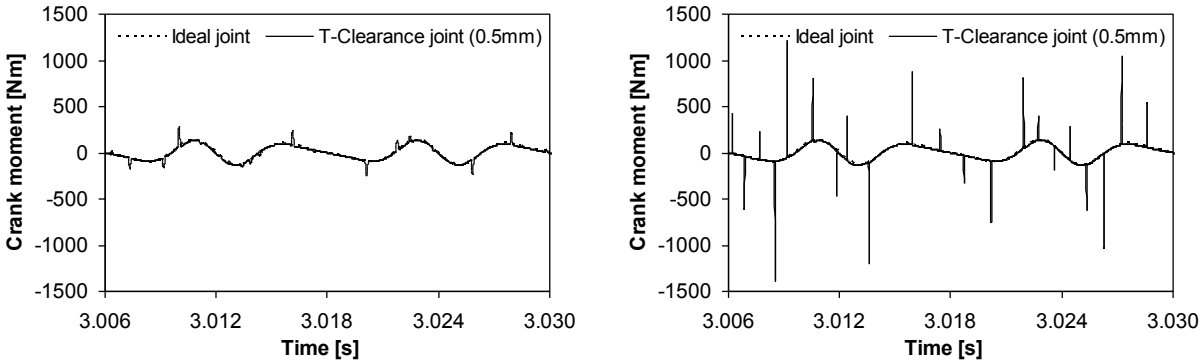

(a) (b)

Fig. 14: Driving crank moment: (a) Lankarani and Nikravesh model given by Eq. (20); (b) Linear contact model for two plane surfaces expressed by Eq. (18).